

# A NEW TYPE OF BALANCED-BRIDGE CONTROLLED OSCILLATOR

R. K. Karlquist

Hewlett-Packard Laboratories  
3500 Deer Creek Rd., MS 26M-3, Palo Alto, CA 94303-1392

## Abstract

*A novel bridge-stabilized crystal oscillator circuit having exceptional temperature stability is described. The contribution to the oscillator temperature coefficient from the circuit components (exclusive of the crystal) is reduced to about  $10^{-11}/^{\circ}\text{C}$ , which is several orders of magnitude better than conventional oscillator circuits. This avoids a situation where the overall tempco is limited by circuit component drift rather than crystal stability, which can easily occur with conventional circuits when the crystal is ovenized at a turnover point. Previous attempts to use a bridge in an oscillator were made by Meacham, who used an imperfectly balanced bridge, and Sulzer, who used a balanced pseudo-bridge. The reasons why these are unsatisfactory are discussed. Although the bridge greatly reduces reactive frequency pulling, it does not directly address the additional issue of pulling due to variations in crystal drive current amplitude. However, it is an enabling technology for a novel ALC circuit with greatly improved stability. The new bridge controlled oscillator is also much less sensitive to other environmental effects such as humidity, power supply voltage, load impedance, and stray capacitance.*

## Introduction

This paper begins with a review of conventional oscillator technology, with particular attention to temperature sensitivity. Next, the bridge stabilized oscillators of Meacham and Sulzer are discussed. This will establish why a new bridge stabilized circuit is needed, what it needs to do, and how it might work. Then the new bridge network and ancillary circuits are described. Within this context, the ALC techniques are developed. Some manufacturability issues and experimental results are presented. The oven and other peripheral hardware used with the oscillator are described in [1].

## Conventional circuits

Virtually all non-bridge-stabilized crystal oscillators are derived from the free-running Colpitts oscillator. In the Pierce oscillator [2], a parallel resonant crystal, replaces the inductor. In the bridged-T<sup>1</sup> (also known as a grounded-base or Butler<sup>2</sup>) oscillator, a series resonant crystal is inserted in series between the emitter and the tank capacitors. (Fig. 1).

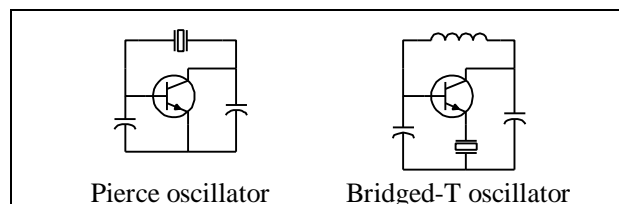


**Figure 1. Basic oscillator circuits.**

In either case, the oscillator consists of an active device (i.e. an amplifier) surrounded by a feedback network that is essentially a crystal filter. The crystal filter will have some phase vs. frequency slope, and the transfer function of the active device will have some phase vs temperature characteristic. Together, these interact so as to make the frequency of oscillation dependent on the active device temperature. The temperature coefficients of the passive components can contribute additional drift.

To minimize the temperature coefficient of such an oscillator, low tempco passives can be used, and the loaded Q of the crystal filter network can be maximized. There are limits to what can be done in these areas. Capacitors are available with a  $\pm 30$  ppm/ $^{\circ}\text{C}$  tempco (NPO), but inductors generally have tempcos of at least a few hundred ppm/ $^{\circ}\text{C}$ . The loaded Q of the crystal network

<sup>1</sup> Not a “bridge” type oscillator, despite the name.

<sup>2</sup> Butler’s “earthed grid” oscillator was actually based on the Hartley, not the Colpitts oscillator [3,5].

can only approach the unloaded Q of the crystal, which is in turn limited by the intrinsic QF product of quartz. If an SC cut crystal is used, a additional problem is created by the need for a high Q mode suppression tank. This tank must have a loaded Q on the order of 10 because the frequencies of mode B and mode C are only about 10% apart. Because of the leverage created by the high Q, the sensitivity of frequency to the value of the mode suppressor components is stepped up an order of magnitude.

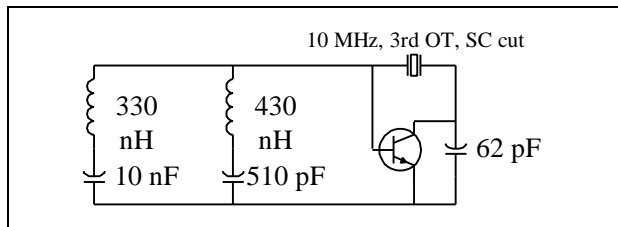


**Figure 2. Pierce oscillator with mode suppressor.**

Fig 2 shows a simplified schematic of a typical 10 MHz third overtone SC cut crystal oscillator [6]. The active device is the commonly used 2N5179. It is derived from the Pierce oscillator of fig 1, with the base-emitter capacitor replaced by the double LC mode suppressor circuit shown. The tempco contribution of the passive components can be calculated using network analysis based on their specified performance. The 2N5179 is not specified for phase and gain vs temperature, so these parameters were measured experimentally with the circuit of fig 3.

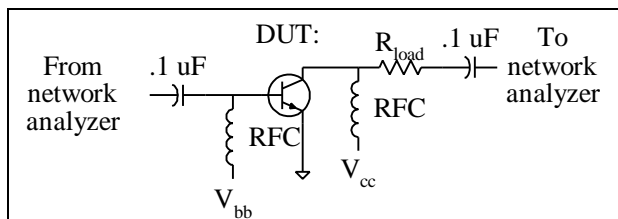


**Figure 3. Transistor tempco test fixture.**

The effect of phase on the frequency of oscillation is obvious, but the effect of gain is indirect. As the transistor temperature changes, the gain (for a given collector current) changes. This gain error must be corrected by the ALC circuit, which typically operates by varying the bias of the transistor. There is a phase coefficient of bias current that then comes into play. No previous example is known of using an independent variable gain element in place of transistor bias for ALC control, but if it were attempted, it would introduce its own

tempco and AM to PM conversion problems, hence be no panacea.

The results of analyzing the circuit of fig 2 are that there are at least six effects that contribute a temperature coefficient on the order of  $10^{-10} / ^\circ\text{C}$  each:

1. Transistor phase shift.
2. Transistor gain shift.
3. 62 pF “NP0” cap ( $\pm 30$  ppm /  $^\circ\text{C}$ ).
4. Inductance tempco ( $+250$  ppm /  $^\circ\text{C}$ ).
5. Inductor Q tempco ( $\Delta Q \rightarrow \Delta L_p$ ).
6. ALC tempco, assuming 0.02 dB /  $^\circ\text{C}$ .

None of these are particularly predictable, they tend to interact, and measurements on real oscillators show these numbers to be optimistic if anything.

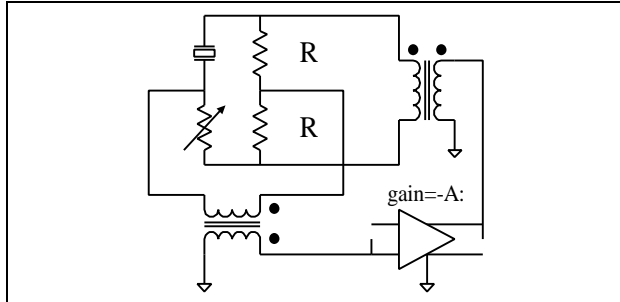
Experimental measurements were made of three complete oscillators of different designs for additional confirmation. The three designs were a conventional Colpitts oscillator, a bridged-T oscillator, and a two transistor Butler oscillator.<sup>3</sup> The Butler oscillator used a transistor array IC instead of 2N5179’s and used a saturated amplifier in place of a conventional ALC scheme. All three oscillators showed a tempco with respect to the active device(s) on the order of  $10^{-9} / ^\circ\text{C}$ . From these results, it was concluded that a breakthrough in tempco reduction of any oscillator of this general class was highly unlikely.

#### The Meacham Bridge Oscillator

The first known attempt to eliminate active device tempco in crystal oscillators was the bridge-stabilized circuit described by Meacham in 1938 [4, 7]. In the Meacham bridge oscillator, the crystal replaces one of the resistors in a Wheatstone bridge (fig 4). The bridge is connected so as to provide negative feedback to the active device at all frequencies except a narrow band around the crystal’s series resonant frequency, where the feedback becomes positive. Note that the bridge must be slightly out of balance at the frequency of oscillation; if it were balanced there would be no feedback to sustain oscillation. The idea is that the frequency of oscillation will be determined by where the bridge balances (or more properly is maximally imbalanced in the positive direc-

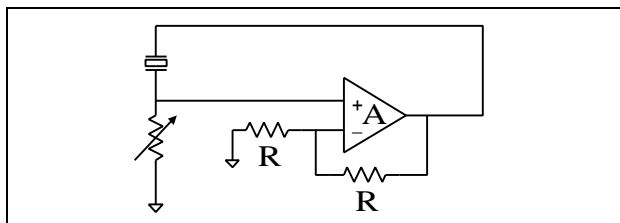
<sup>3</sup> Not the oscillator described in [5], rather Butler’s previous “two-valve” design.

tion), rather than the phase shift through the active device



**Figure 4. Meacham bridge-stabilized oscillator.**

Meacham showed that indeed the circuit becomes less sensitive to perturbations outside the bridge as the gain of the active device increases, which causes the bridge to operate closer to being balanced. He described this circuit as a sort of Q-multiplier, which makes the Q of the crystal appear to increase by a factor equal to the amount of excess gain in the active device. The increase in effective Q makes the crystal harder to pull off frequency. Although he didn't publish any tempco measurements, his oscillator achieved long term aging of  $10^{-9}$ /day, which seems promising considering that the active device was a directly heated triode.



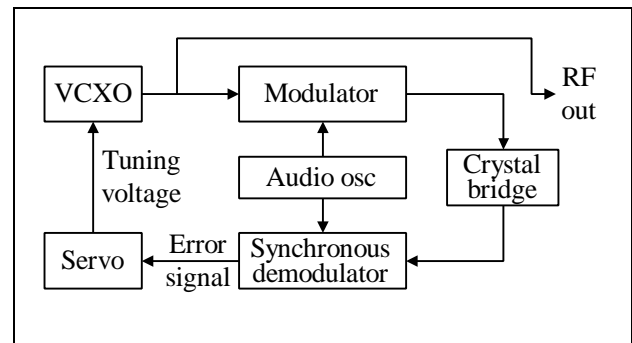
**Figure 5. Meacham oscillator utilizing op amp**

Fig 5 shows another way of looking at Meacham's circuit [8]. Here it can be seen that what is really going on is that negative feedback has been applied to the active device as if it were an op amp. And this is the key to understanding the limitations of the Meacham bridge oscillator. For any frequency not in the vicinity of the crystal resonant frequency, the crystal can be considered an open circuit, and the conditions for stability of the active device are the same as for an op amp with a closed loop gain of -1. This requires that the active device be equivalent to an op amp that is unity-gain stable. It is extremely difficult to realize a unity-gain op amp using conventional dominant pole compensation

with a gain bandwidth product of more than about 300 MHz. This limits the active device gain at 10 MHz to about 30 dB. Since 6 dB of this gain is necessary to overcome the voltage drop through the crystal, only 24 dB of negative feedback is being applied. This is not a sufficient amount of feedback to remove the dependence on the phase shift of the active device.

One way to overcome this limitation is to change the compensation from a dominant low pass pole to a dominant band pass complex pole pair. This could be implemented, for example, by shunting the input with a parallel LC tank. However, the tempco of the tank components creates a new source of drift. This dilemma is a general problem that would apparently occur with any scheme involving the use of negative feedback to stabilize the active device. The arguments presented here are similar to the reasons why active filters are never used at 10 MHz, at least if a high degree of precision and stability is required of them.

Even if all of the above problems could be overcome, an additional problem with the Meacham bridge oscillator is that the mode suppressor required for SC cut crystals would have to be inside the bridge, hence it would have just as high a tempco as it would in a non-bridge circuit.



**Figure 6. Bridge servo'ed oscillator.**

#### Bridge servo'ed oscillators

In the early 1950's, there were experiments with stabilizing a crystal oscillator by using an auxiliary crystal in a bridge circuit operating in balance. [9] The idea was that a servo loop would tune the oscillator to keep the bridge balanced, which would force the frequency of oscillator to coincide with the resonant frequency of the crystal at all times (fig. 6). The bridge was

the same modified Wheatstone bridge used in the Meacham oscillator, and the servo loop was a conventional lock-in amplifier operating via synchronously detected audio modulation as commonly used in atomic standards. The advantage of this scheme is that the bridge could operate with arbitrarily small deviation from balance and there was no limit to the servo loop gain. The obvious disadvantage was the requirement for two crystals.

#### Sulzer's "bridge-balancing" oscillator

In 1955, Sulzer [10] described an oscillator and bridge using a single crystal that servo'ed the frequency so as to maintain bridge balance (fig 7). The basic bridge is again the modified Wheatstone bridge. Instead of driving the bridge with a separate VCXO, the crystal in the bridge is made part of an oscillator circuit. The output of the active device used as the oscillator drives the top of the bridge, the same as the VCXO would in the figure 6. The input of this oscillator is driven by feedback from the bridge. The proper output port of the bridge cannot be used because it has a null, not a peak, at resonance. Instead, the amplifier input is connected in shunt with one of the bridge resistors. A lock-in amplifier is used to servo the bridge into balance, but the audio modulation is cleverly added by modulating the impedance of the bridge, instead of by adding undesirable sidebands to the oscillator signal. This was done with an electromechanical chopper relay.

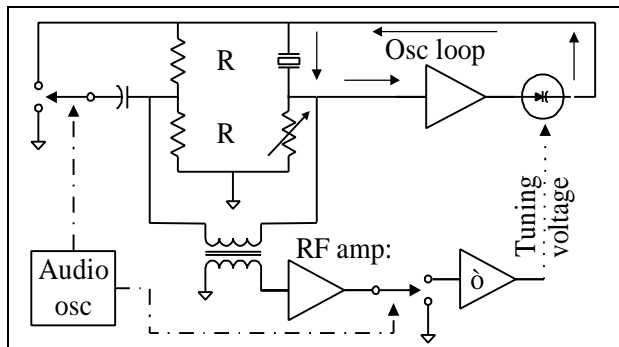


**Figure 7. Sulzer bridge-balancing oscillator.**

The basic problem with this design is that the integrity of the bridge is violated due to the shunt loading of the arms by the oscillator active device and the modulator. There are other implementation problems. The active device must present a high impedance load to the bridge, which compromises phase noise. In a modern

design, the mechanical chopper would have to be replaced by some sort of electronic equivalent, such as FET switches, which would add their own capacitive loading across the bridge. Finally, there would inevitably be crosstalk between the bridge modulator and oscillator sections that would impress audio sidebands on the output signal at some level. Although Sulzer was able to demonstrate greatly reduced sensitivity of the frequency to such perturbations as power supply voltage, this design clearly left a lot to be desired.

#### The ideal bridge-stabilized oscillator

The previously described oscillators each have unique advantages and disadvantages. What is needed is an ideal bridge stabilized oscillator that combines all the advantages with none of the disadvantages by meeting the following requirements:

1. One crystal is used for both the bridge and the oscillator.
2. The bridge operates at balance and controls the frequency of oscillation.
3. The integrity of the bridge is maintained.
4. No audio modulation is added.
5. Low phase noise is facilitated.
6. Overtone and mode control can be effected outside the bridge and without compromising stability.

#### A true balanced-bridge controlled oscillator

The approach chosen to meet these requirements is shown in fig 8. The crystal is removed from a VCXO and embedded in a two port bridge network. Meanwhile, port 1 of the network is connected to the VCXO in place of the crystal. A null detector operates an AFC (automatic frequency control) loop. The key is to devise a two-port bridge network that meets two requirements: (1) The transfer function from one port to the other has a null output when the crystal is excited at resonance (as in the modified Wheatstone bridge) and (2) Port 1, the input, has a driving point impedance such that it emulates the impedance of a freestanding crystal (i.e. the bridge is "transparent"). Transparency, as used here, means that if the oscillator were connected to port 1 of the network, it would operate just as if it were connected directly to a crystal. In other words, port 1 emulates a virtual crystal. The modified Wheatstone bridge originated by Meacham is not transparent because of the

shunting effect of the resistors on the non-crystal side of the bridge

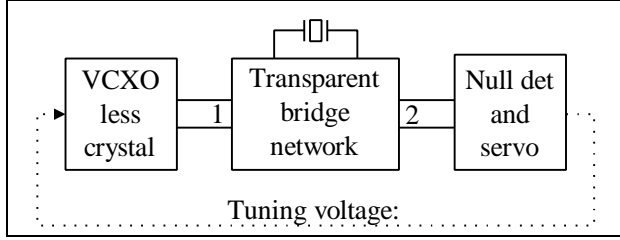


**Figure 8. Balanced bridge controlled oscillator**

Development of the bridge network

Although the bridge network does not require any particular oscillator design for its proper operation, some initial assumptions will be made about the oscillator to facilitate the analysis. The oscillator will be assumed to be of the series resonant type, and will be assumed to have some sort of ALC system that maintains constant (virtual) crystal current. Thus, when port 1 of the bridge network is substituted for the crystal, the oscillator will then maintain constant current into port 1. Also, the holder capacitance ( $C_0$ ) of the crystal will be assumed to be negligible at this time. These assumptions will be revisited after the basic bridge network is determined. An additional assumption is that the output port can be considered to be unloaded because the input admittance of the null detector is negligible.

The network will be analyzed with  $z$  parameters. Since  $i_2 = 0$ , the driving point impedance at port 1 is the same as  $z_{11}$  by definition.<sup>4</sup> The desired driving point impedance of the bridge network is of the same form as a crystal (without  $C_0$ ), hence  $z_{11} = [(Q_v/\omega_0)s^2 + s + Q_v\omega_0](R_v/s)$ , representing a virtual crystal<sup>5</sup> with motional resistance  $R_m = R_v$ , quality factor  $Q_m = Q_v$ , and resonant frequency of  $\omega_0$ . The desired form of  $v_2$  vs frequency is a null at resonance. Since  $i_1$  is constant (due to oscillator ALC),  $v_2/i_1$  should also be of this form. And because  $i_2 = 0$ ,  $z_{21} = v_2/i_1$ . A null at resonance can be implemented simply by a complex pair of zeros on the  $j\omega$  axis at  $\pm j\omega_0$  (complemented by poles at 0 and  $\infty$  for

<sup>4</sup> The  $z_{11}$  parameter is defined as the driving point impedance of port 1 with port 2 open.

<sup>5</sup> Denoted by the  $v$  subscript.

realizability.) Hence,  $z_{21} = (s^2 + \omega_0^2)(K/s)$ , where  $K$  is a gain constant to be chosen later. The bridge will not utilize non-reciprocal elements, therefore  $z_{12} = z_{21}$ . The remaining  $z$ -parameter,  $z_{22}$ , is not constrained, so it is advantageous to set  $z_{22} = z_{11}$  so that the network is of the more easily realized symmetrical class.

Network theory predicts that if a symmetrical two-port is realizable in any form, it is realizable as a balanced lattice network. Furthermore, a balanced lattice network is actually a form of bridge circuit. Hence if a lattice solution can be found, a bridge solution has been found. For a balanced lattice network with known  $z$ -parameters, the impedances of the straight through arms,  $z_a$ , and the crossover arms,  $z_b$  are given by standard formulas [11] as follows:

$$z_a = z_{11} + z_{21} = [(Q_v/\omega_0)s^2 + s + Q_v\omega_0](R_v/s) + (s^2 + \omega_0^2)(K/s) \\ = [(Q_v/\omega_0 + K/R_v)s^2 + s + (Q_v/\omega_0 + K/R_v)\omega_0^2](R_v/s)$$

$$z_b = z_{11} - z_{21} = [(Q_v/\omega_0)s^2 + s + Q_v\omega_0](R_v/s) - (s^2 + \omega_0^2)(K/s) \\ = [(Q_v/\omega_0 - K/R_v)s^2 + s + (Q_v/\omega_0 - K/R_v)\omega_0^2](R_v/s)$$

By setting arbitrary gain constant  $K = R_v Q_v/\omega_0$ , the crossover arms are reduced to  $z_b = R_v$ . The straight through arms become  $z_a = [(2Q_v/\omega_0)s^2 + s + 2Q_v\omega_0](R_v/s)$ , which, like  $z_{11}$ , represents the impedance of a crystal resonant at  $\omega_0$  with  $R_m = R_v$ , but with a doubling of  $Q_m = 2Q_v$ , which also implies a doubling of  $L_m$  and a halving of  $C_m$ . The resulting lattice is shown in fig. 9. The network will appear to the oscillator as a crystal with half the  $q$  of the actual crystals. This minor deviation from the original transparency requirement is tolerable and is not an obstacle to the ultimate objective.

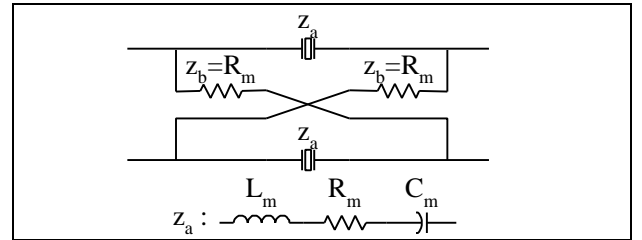


**Figure 9. Theoretical transparent crystal bridge.**

Having chosen  $K = R_v Q_v/\omega_0$ , it follows that  $z_{21} = (s^2 + \omega_0^2)(R_v Q_v/\omega_0 s)$  which results in a sensitivity on a fractional frequency basis at the null detector of  $|z_{21}| = 2R_v Q_v \omega_0 (\Delta\omega_0/\omega_0) = (1/C_m)(\Delta\omega_0/\omega_0)$ , where  $C_m$  is the motional capacitance of the crystal.

A matched pair of crystals (or perhaps a monolithic dual resonator) would be required to build this lattice. This problem of component duplication comes up frequently in crystal filter design and can be solved in this case by using the standard filter technique of converting the balanced lattice to a half lattice consisting of the crystal, a resistor and a transformer (fig. 10) [12]. The half lattice also has the advantage of having ports that can be used in either balanced or unbalanced mode. The resistor, matched to  $R_m$ , will be referred to as the image resistor.

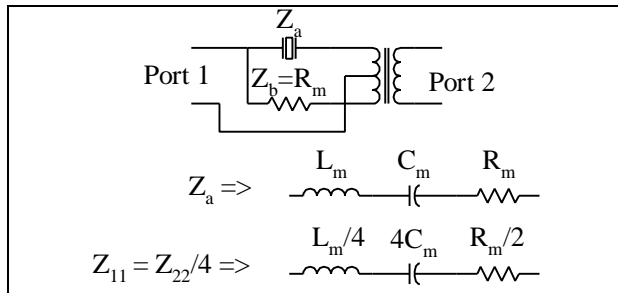


**Figure 10. Practical transparent crystal bridge.**

The conversion to a half lattice has the side effect of transforming the impedance level at port 1 down by a factor of 4. The impedance level at port 2 is unchanged if the turns ratio of the transformer is 1:1, although any ratio can be used, subject to constraints caused by implementation details. Because of the symmetry of the network, the ports are interchangeable allowing port 2 to be connected to the oscillator with port 1 connected to the null detector. The apparent impedance of the crystal can then be transformed up or down to suit the oscillator. If desired, the imbalancing effects of the crystal holder capacitance,  $C_0$ , can be compensated out by adding an equal shunt capacitance across the image resistor.

#### Development of a null detector

The first requirement for the null detector is that it have a high input-impedance front end to avoid drawing significant current from port 2. In practice, it is sufficient to have an input impedance about an order of magnitude higher than the magnetizing inductance/impedance of the transformer, which will be a few thousand ohms at most. If the null detector simply consisted of a buffer amplifier driving a scalar power detector, it could detect the presence or absence of a null, but

not the sign of the frequency error. That would require using audio modulation to sweep across the null as in previous schemes. Sign information would be essential to any servo loop.

To obtain sign information without resorting to auxiliary modulation, a vector type detector operating at the crystal frequency must be used. A vector detector requires a phase reference, and port 1 of the bridge is the obvious choice. A vector voltmeter connected to ports 1 and 2 could be made to work after a fashion as a null detector, but has the problem that the phase slope reverses outside the 3 dB point of the crystal, which would cause convergence problems. Also, the voltage at port 1 varies widely in amplitude. On the other hand, the current at port 1 is constant, and its relationship to the voltage at port 2 is given by  $z_{21}$ , a function having the ideal form to steer a servo loop. If it were easy to compute the quotient  $z_{21}$ , the problem would be solved. Unfortunately, division is difficult to implement using analog computer techniques at RF.

However, in the time domain, the following observations can be made. Assume that the ALC fixes  $i_1$  at  $I_X \cos \omega t$ , where  $I_X$  is the magnitude of the virtual crystal current (twice the actual crystal current). Then  $v_2 = I_X z_{21} = I_1 (1/C_m) (\Delta\omega_0/\omega_0) (-\sin \omega t)$ . Now if  $i_1$  retarded by 90 degrees, i.e.  $-\sin \omega t$ , is multiplied by  $v_2$ , the result is  $(I_X^2/C_m) (\Delta\omega_0/\omega_0) (\sin^2 \omega t) = (I_X^2/C_m) (\Delta\omega_0/\omega_0) (1 - \cos 2\omega_0 t)/2$ , which has the DC component  $(I_X^2/2C_m) (\Delta\omega_0/\omega_0)$ . The multiplication is implemented by a Gilbert multiplier, with the LO port driven by a phase-retarded voltage corresponding to  $i_1$ . This provides a constant amplitude LO signal, since  $I_1$  is stabilized by the oscillator ALC. The RF port of the multiplier is driven by  $v_2$  with about 30 dB of gain added by the AFC RF amplifier. The DC output of the multiplier is then extracted by a low pass filter (fig. 11). The multiplier will be referred to hereafter as the synchronous demodulator because its operating conditions are more similar to conventional synchronous demodulators than phase detectors. A capacitor is inserted in series with port 1 of the bridge to convert  $i_1$  to a voltage with an inherent 90° phase lag. Ideally, the voltage directly across the capacitor would be utilized. However, it is much easier to use the voltage from the capacitor to ground. If  $X_c \gg z_{11} = R_m/2$ , the phase error contributed by  $v_1$  will be negligible. An emitter follower buffers this voltage to

drive the LO port of the multiplier. The emitter follower also drives the ALC detector of fig. 13 that is described below. The reactance added by the port 1 series capacitor is cancelled out by an inductor of equal and opposite reactance.

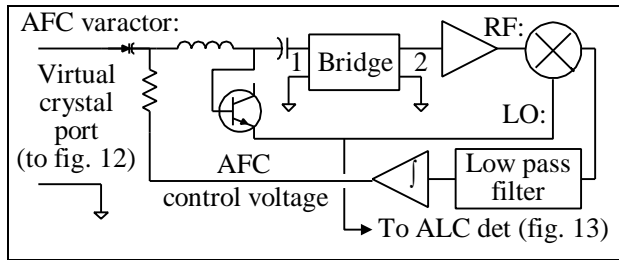


**Figure 11. AFC system block diagram.**

#### AFC loop design

The DC output from the synchronous demodulator drives a lead-lag type integrator (fig 11) that controls the bias (details not shown) of the AFC varactor, which is in series with port 1. The operation of the servo loop pulls the frequency of oscillation up or down as necessary to keep the bridge balanced. This varactor has no effect on the frequency at which the bridge balances, but it does modify the resonant frequency of the virtual crystal and hence pulls the frequency of any oscillator connected to the bridge. It is convenient to set the value of the inductor in series with port 1 so that the combined reactance of the AFC varactor, inductor, and capacitor is zero when the AFC voltage is at mid-range. A loop time constant of about 1 second is used in the AFC loop which results in no measurable noise modulation of the oscillator by the AFC loop. In the event there is an abrupt perturbation to the oscillator (such as a step in the power supply voltage), a recovery time of a few seconds is necessary for the AFC loop to return the frequency to its original value [15].

#### Automatic level control (ALC)

In a precision crystal oscillator, the crystal drive current must be very well stabilized, because the crystal exhibits a significant amplitude to frequency (AM/FM) conversion coefficient due to nonlinearities inherent in the quartz. Fig. 12 shows the AM/FM curve, as measured in the oscillator described in this paper, by adjusting the ALC set point. The design goal was to hold the drive current stable to 0.0002 dB/°C, resulting in a tempco contribution of about  $10^{-12}/^{\circ}\text{C}$ .

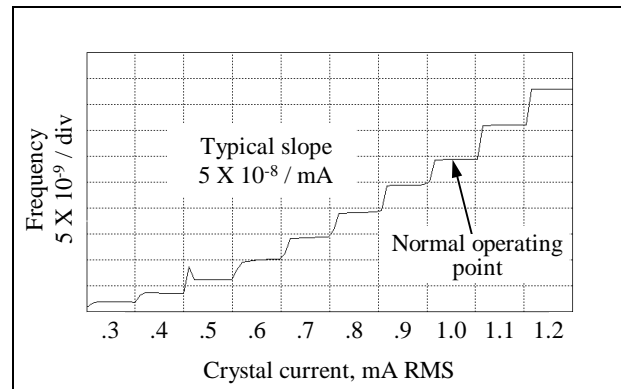


**Figure 12. Drive level induced frequency shift.**

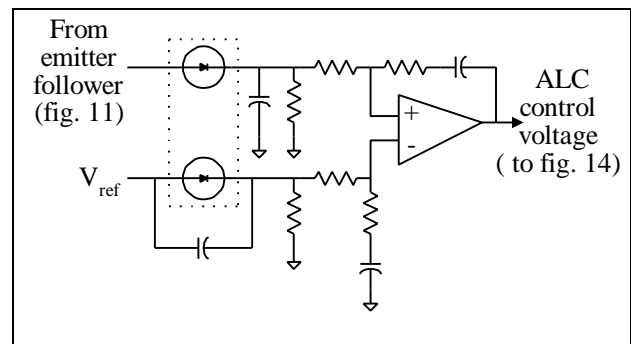


**Figure 13. ALC detector.**

A diode peak detector was chosen as the basis for the ALC detector because it is certainly the simplest method, and is probably as temperature stable as any method. Fig 13 shows a conventional temperature compensated detector. A matched pair of thermally coupled diodes is used, one acting as an RF peak detector, the other as a DC reference subtracted from the rectified output. Ideally, the  $\approx -2\text{mV}/^{\circ}\text{C}$  tempcos are equal and cancel each other out. The compensation can never be perfect, even for perfectly matched diodes at identical temperatures, because the diodes operate under the different conditions of pulsed current vs steady state current. The temperature induced offset error in the detector system mainly consists of this residual tempco mismatch. In practice, this mismatch, for reasonable DC bias currents, is about 1/2%, corresponding to  $10 \mu\text{V}/^{\circ}\text{C}$ . For a given rectified DC output current, the residual tempco is not very sensitive to input voltage amplitude. Linearity and frequency response, traditionally an im-

portant issue with diode detectors are irrelevant here since the amplitude and frequency are constant.

Thus it can be concluded that the error in the detector is dominated by offset voltage tempco. Since the absolute error doesn't increase significantly with amplitude, the amount of error relative to the voltage being measured is inversely proportional to that voltage. I. E., a  $10\ \mu\text{V}$  error in measuring a  $.1\text{V}$  signal represents  $0.001\ \text{dB}$ , while a  $10\ \mu\text{V}$  error measuring a  $1\text{V}$  signal represents  $0.0001\ \text{dB}$ . Therefore, if a temperature stable way of stepping up the voltage to be measured can be devised, the effective ALC stability can be improved.

The potential for such a method already exists in the circuit of fig. 11. By making the capacitor in series with port 1 very small, the voltage at the emitter follower can be made arbitrarily large. Of course, the series inductor has to be increased to compensate for the capacitor change. The temperature stability of the step up ratio can be guaranteed by using an NPO capacitor. The emitter follower has a negligibly low tempco of gain because it is lightly loaded. The emitter follower in fig. 11 drives the diode detector of fig. 13, which is used to control the gain of the oscillator shown in fig. 14 as discussed below. The ALC integrator has standard lead-lag compensation and a time constant of about  $.1$  second.

The use of a bridge to control the oscillator is essential as an enabling technology for the stepped up voltage ALC technique.<sup>6</sup> If it were attempted in an ordinary oscillator, the high temperature sensitivity of the compensating inductor in series with the step up capacitor would greatly degrade the stability of the oscillator, making the method unusable.

#### The oscillator proper

At this stage, the oscillator itself is almost an afterthought. The bridge should be compatible with most series resonant crystal oscillators. A bridged-T oscillator was chosen for this design (figs 1,14), because it is the simplest possible oscillator circuit for overtone SC cut crystals. A single pi-network tank provides feedback, overtone selection, and undesired mode suppression. By making the Q of the tank at least 10, it suppresses undesired mode B oscillations at  $10.95\ \text{Mhz}$ , making an explicit mode suppressor superfluous.

<sup>6</sup> Patented [15].

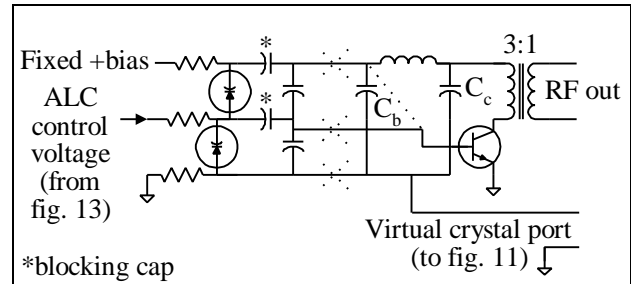


**Figure 14. Bridged-T oscillator with gain control.**

Fig. 14 shows a simplified schematic of the oscillator proper. The circuit is based on the simple bridged-T oscillator of fig. 1, but has two modifications. The virtual crystal represented by the bridge (fig. 11) replaces the actual crystal, and the base now gets its feedback through the capacitive voltage divider rather than directly from  $C_b$ . The dotted lines show the original topology of fig. 1. The capacitive voltage divider is utilized by the ALC system, as described below.

#### Oscillator gain control

The oscillator must have a gain control input to connect to the ALC integrator. Typically, this is done by varying the oscillator collector current. While it is clearly the simplest method, it requires that the oscillator run in a starved bias condition that increases distortion, and it is difficult to get a lot of dynamic range while keeping collector current within reasonable limits. Another problem is that collector current tends to get out of control at turn on, and can cause oscillator starting problems. In a bridge controlled oscillator, extra dynamic range in the ALC is needed to maintain oscillation during AFC acquisition.

To address all of these ALC issues, the variable capacitive voltage divider in fig. 14 was used. A portion of the base capacitance has been replaced with a capacitive voltage divider made from two varactors. The base operates from the divided down feedback voltage, hence the division ratio controls the loop gain. The division ratio is controlled by the ALC control voltage, which causes the bias voltages of the two diodes to move in opposite directions as the control voltage varies. Thus at low ALC voltage, the upper capacitor has high voltage, hence low capacitance and high reactance. The lower capacitor has low voltage, hence high capacitance and low reactance. This causes the base voltage to be a small fraction of the voltage across  $C_b$ . The situation is re-



versed at high ALC voltage resulting in most of the  $C_b$  voltage being available at the base.

If varactors with a  $\gamma = 1$  characteristic are used, the equivalent capacitance of the two diodes in series is invariant as the ALC voltage is varied. However, varactors having sufficiently high capacitance for this application are only available with a  $\gamma = 2$  characteristic. Shunt capacitors (fig. 14) can be added to the varactors to “linearize” them fairly effectively in the sense that the series equivalent capacitance is constant to within a few percent over the ALC range. This together with the desensitizing effect of  $C_b$  results in a design where the total base capacitance is nearly independent of ALC voltage. Thus, the ALC loop does not significantly affect the AFC loop; i.e. inducing a change in ALC voltage by adding extra loading to the oscillator has a negligible effect on AFC voltage. The reverse is not true; when the AFC control voltage is at one of the rails (maximum pulling), the ALC control voltage rises substantially to counteract the inevitable gain rolloff that accompanies frequency pulling.

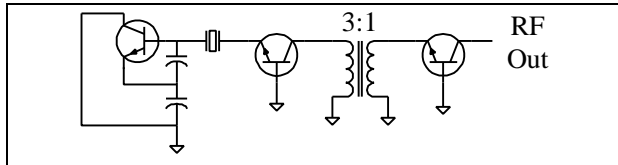


**Figure 15. Burgoon low phase noise output circuit.**

#### Extracting the output

Fig. 15 shows a conventional crystal oscillator with an output scheme having the lowest possible phase noise floor. [6,13] The right hand terminal of the crystal would normally go to ground in a Pierce configuration. Instead it is returned to ground through the very low input impedance of the grounded base amplifier, thus only minimally disrupting normal oscillator operation. Many kHz from the frequency of oscillation, where the phase noise floor is reached, the crystal impedance is so high as to essentially constitute an open circuit. Open circuiting the emitter eliminates base-recombination current noise, leaving only collector shot noise current. The output of the first grounded base amplifier is then stepped up so that it dominates any subsequent buffer amplifiers.

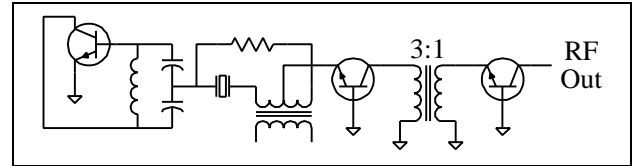


**Figure 16. Output adaptation to bridge oscillator.**

Fig 16 shows a way to adapt this technique to the bridge controlled oscillator. In this case, the transformer center tap, which normally goes to ground, now returns to ground through the input impedance of the grounded base transistor. This topology is certainly usable, but it does have the disadvantage that the buffer amplifier must be colocated with the oscillator. Also, there is some risk that the extra impedance in series with the center tap could be detrimental to the accuracy of the bridge.

The method actually used, however, was to place the load in series with the collector of the oscillator transistor, using a current transformer to make the load appear to be floating (fig. 14). This can then be used to drive subsequent grounded base amplifier. It can be shown that this configuration, like the ones of figs. 15 and 16, also has optimally low phase noise due to lack of base recombination current noise. There are only two connections from the oscillator in fig. 14 to RF ground: The emitter and the virtual crystal port. Since this port emulates a crystal, it, too, is effectively an open circuit at phase noise floor frequencies. Since nothing else in the circuit has any RF path to ground either, the emitter, which is grounded, has no RF path back to the base or collector. Therefore, for noise purposes, the emitter is open circuited, thus eliminating base recombination current. It should be noted that the bridge circuit is an enabling technology for this technique; otherwise the transformer would degrade the tempco.

The output impedance at the secondary is fairly high because of the high output impedance of the transistor. If it is used to drive a grounded base amplifier, that amplifier will effectively be driven by a current source and therefore have no base recombination noise. The current transformer triples the secondary current so that the oscillator shot noise dominates over any subsequent grounded base buffer amplifier shot noise.

#### Electronic frequency control (EFC) capability

For many applications it is desirable to have EFC capability so that the oscillator can be used in VCXO mode. A method of doing this is shown in fig 17. Note that the EFC varactor located inside the bridge should not be confused with the AFC varactor located outside the bridge. The EFC varactor changes the frequency at which the bridge balances. The AFC varactor is used to force the oscillator to oscillate at this bridge balance frequency. The crystal resonant frequency can be pulled above series resonance in a straightforward manner by adding series capacitance with the EFC varactor and/or  $C_{up}$ , a “pull up” capacitor that can be used to remove crystal calibration frequency error. The bridge enables an additional unique feature. A “pull down” capacitor,  $C_{down}$ , in series with the image resistor allows tuning below series resonance. The operation of the bridge makes the pull down capacitor behave as if it added negative load capacitance to the crystal; hence it has the unusual property of decreasing the frequency as its value decreases. This technique was previously applied to a Meacham bridge oscillator [13].

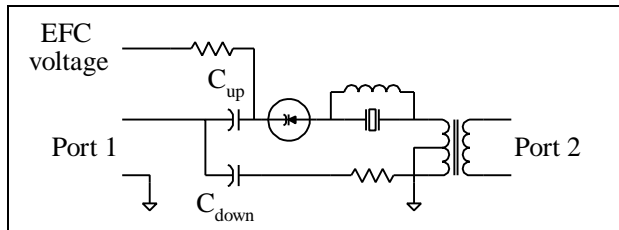


**Figure 17. Adding EFC to bridge.**

In practice, if the crystal has been fabricated to be series resonant at the exact design frequency, the pull down capacitance is chosen to be equal to the varactor capacitance at mid-range, and the pull up capacitor is increased to an effectively infinite value. Then at mid range, the varactor and pull down capacitor balance out and the bridge balances at series resonance. It can then be tuned equal amounts above and below resonance as the EFC voltage is varied. If the crystal has a frequency calibration error, it can be corrected by changing the values of  $C_{up}$  and  $C_{down}$  appropriately.  $C_{up}$  acts as a conventional trimmer and pulls the frequency *higher* as it gets *smaller* while  $C_{down}$ , unlike conventional crystal trimmer capacitors, pulls the frequency *lower* as it gets *smaller*.

#### EFC varactor tempco

Varactors have a typical capacitance tempco of 500 ppm/°C. If the maximum varactor pulling is 10 Hz, this will result in a frequency tempco of  $5 \times 10^{-10}/^{\circ}\text{C}$ . This is much worse than the rest of the oscillator, so it is essential to plan on collocating the EFC varactor with the crystal to obtain high thermal gain.

#### Bridge balance issues

The problem of balancing the bridge involves two degrees of freedom: The crystal must be at series resonance to remove any reactive imbalance, and the image resistor must match the ESR of the crystal to remove any resistive imbalance. In practice, the AFC loop has no difficulty servo'ing out the reactive imbalance by controlling the frequency. The resistive imbalance must be dealt with on an open loop basis. The ESR of crystals varies somewhat from unit to unit and is also has a moderate dependence on temperature and even a slight dependence on drive level. As a practical matter, then, the image resistor needs to be adjustable so that the bridges in oscillators can be resistively balanced on an individual basis. This adjustment is made by setting the image resistor adjustment such that the signal at the RF input of the multiplier reaches a null. This null must at least be good enough to avoid exceeding the dynamic range of the multiplier. It becomes more critical as the gain of the RF amplifier increases, which puts a practical limit on gain.

The bridge balance is affected somewhat by the value of the EFC voltage, because the ESR of the varactor is a function of bias voltage. However, this effect can be reduced to an acceptably low amount (equivalent to an image resistor error of about 1 ohm) by proper choice of varactor, component values and topology in the bridge.

It is theoretically possible to add another servo loop in quadrature to automatically achieve resistive balance. This loop would have the same architecture as the AFC loop, except that the 90° phase shift of the LO would be omitted and the loop control voltage would operate a variable resistance element, such as a PIN diode, in series with the image resistor. This concept has not been tried experimentally.

#### Principal error sources

The main cause of frequency drift in the bridge controlled oscillator is the combination of image resistor error and AFC phase error. Image resistor error, discussed above, results in an error signal at the output of the bridge that cannot be servo'ed out by the AFC loop. If the multiplier inputs are in exact quadrature with respect to the  $i_1$  and  $v_2$  of the bridge, the AFC loop will respond only to reactive bridge imbalance and will have zero sensitivity to resistive bridge imbalance caused by image resistor error.

The problem comes about when both image resistor error and phase error are present. With respect to the AFC loop behavior, a phase error of  $\mathbf{f}$  at the multiplier effectively adds a phase shift of  $\mathbf{f}$  to the impedance of the bridge components. Thus, an image resistor error (denoted  $\Delta R$ ) will be converted to a partially reactive error. For example, if  $\Delta R = 1$ , and the  $\mathbf{f} = 6^\circ$ , there will appear to be an additional reactance of  $1 \sin 6^\circ = .1$  ohms in series with the crystal. The AFC loop will "correct" the apparent reactive imbalance by shifting the frequency to create an actual reactive imbalance of equal and opposite value, resulting in a frequency error. In the example, the frequency error will be equal to whatever pulling effect .1 ohms of reactance would normally have on the crystal. The frequency error (Hz) is given by  $f_{\text{error}} = (\mathbf{Dr})(\mathbf{f})/(720L_m)$  where  $\mathbf{Dr}$  is the resistive imbalance (ohms),  $\mathbf{f}$  is the phase error ( $^\circ$ ) and  $L_m$  is the crystal motional inductance (H). For the crystal used in this oscillator,  $L_m = .7H$ , resulting in an error of .01 Hz/ohm for a  $5^\circ$  phase error.

An alternate description of this problem can be made along the lines of the Q multiplication discussion in [7] as follows: For the crystal used here  $R_m = 40$  ohms, hence  $Q_u = 1.1$  million at 10 MHz, which implies a frequency shift of .4 Hz for a  $5^\circ$  phase shift. This is 40 times as much frequency shift as would be caused by  $5^\circ$  phase error at the synchronous demodulator with  $\Delta R = 1$  ohm. This is equivalent to a Q multiplication of 40:1 which the ratio:  $R_m/\Delta R = 40/1 = 40$ . A critical difference here is that there is no fundamental limitation to how much Q multiplication is possible.

The effective phase error can be easily measured on an oscillator by making a slight adjustment of the image resistance pot. The frequency before vs after adjustment is measured with a counter and compared to the

the pot resistance before vs after as indicated on an ohmmeter.

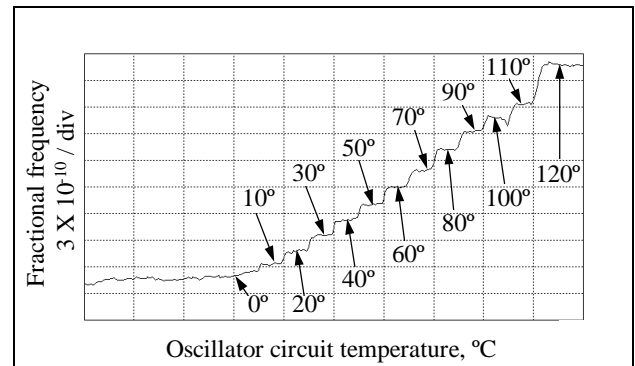
Since the object is to build an oscillator, not a network analyzer, stability is the primary objective., as opposed to absolute accuracy. To this end, it is relevant to take the temperature derivative of the frequency error equation introduced above:

$$\begin{aligned} df_{\text{error}}/dT &= d/dT [(\Delta R)(\phi)/720L_m] \\ &= [d\Delta R/dT][\phi]/720L_m + [\Delta R][d\phi/dT]/720L_m \end{aligned}$$

Resistive balance in a bridge should be relatively insensitive to temperature assuming quality resistors are used. The implication of this with respect to the first term above is that it is probably not worth the effort to accurately adjust the phase error to exactly zero. On the other hand, the phase shift at 10 MHz in the ALC RF amplifier is probably always going to be somewhat temperature sensitive. The implication of this with respect to the second term is that it is worth some effort to minimize the image resistor error, especially since it has to be adjusted anyway.

### Experimental results

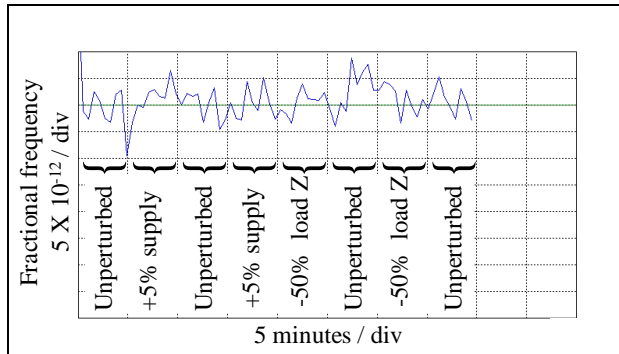
To check the repeatability of the oscillator design, the same crystal was installed in 25 different oscillators boards. The frequencies of oscillation all fell within  $5 \times 10^{-8}$ .



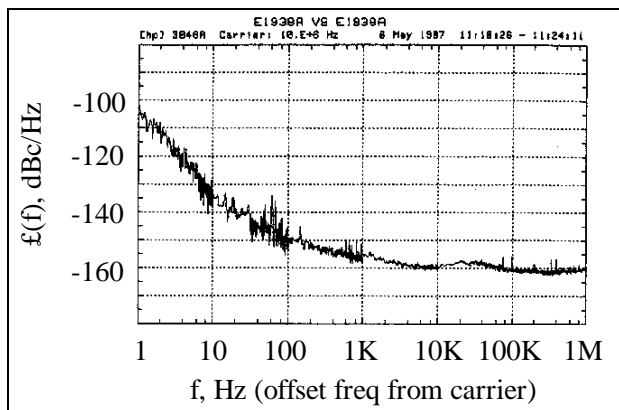
**Figure 18. Oscillator circuit tempco (less crystal).**

Fig. 18 shows the frequency vs. temperature of a typical oscillator, with a tempco of about  $2 \times 10^{-11}/^\circ C$ . Some oscillators have been better than  $10^{-11}/^\circ C$ . In this measurement, the crystal and oscillator were ovenized in separate ovens, and the set point of the oscillator oven only was incremented. No EFC varactor was installed

during these temperature tests. Fig. 19 shows the unmeasurably high immunity to changes in output loading, and power supply voltage. These tests were performed directly on the oscillator circuit with no intervening buffer amplifier and no voltage regulators (except for the ALC reference voltage).



**Figure 19. Power supply and load impedance effects.**



**Figure 20. Phase noise.**

Fig. 20 shows the measured phase noise. The close in phase noise is comparable to a conventional oscillator using a similar crystal. The phase noise floor of at -160 dBc/Hz (which includes a buffer amplifier) is reasonable for this class of oscillator, but theoretical noise calculations indicate it is capable of being improved about 10 dB by optimizing the output transformer. Fig. 21 shows the short term stability. Again, this is comparable to a conventional oscillator using a similar crystal. The rise around 10 to 100 seconds is believed to be due to the measurement system. Hence there is experimental verification that the AFC loop is not adding significant noise modulation to the oscillator.

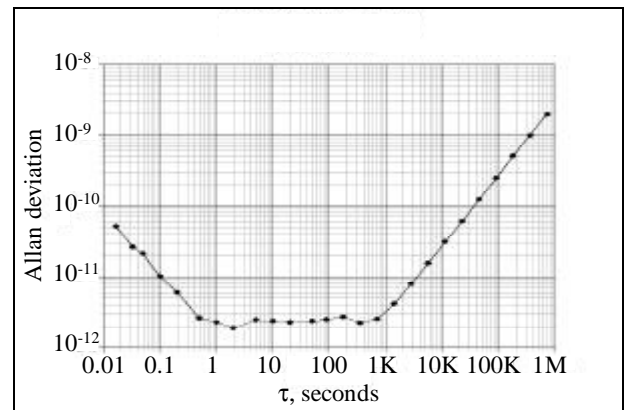


**Figure 21. Short term stability.**

#### A comment on complexity

The oscillator described here may seem to have the disadvantage of being more complex than a conventional oscillator. Additional circuitry consisting of the bridge, RF amplifier, Gilbert multiplier and AFC integrator has been added. However, no ovenized buffer amplifiers or voltage regulators are necessary. The AFC integrator can be half of a dual op amp, the other half being the ALC integrator. Therefore, the increase in complexity is not severe. In the implementation used here, the oscillator occupied about 16 cm<sup>2</sup> (2.5 in<sup>2</sup>) of space on its PC board, not counting the crystal.

#### Conclusions

A practical technique for controlling the frequency of a crystal oscillator with a bridge has been described. The high performance of this technique has been demonstrated. Critical design issues have been outlined along with methods of resolving them.

#### Acknowledgments

Len Cutler suggested some tests for possible sources of error. Robin Giffard supplied a dual transistor Butler oscillator for testing. Jack Kusters and Lee Cosart assisted with characterization.

### References

- [1] R. K. Karlquist, et al, "A Low Profile High Performance Crystal Oscillator for Timekeeping Applications," Proceedings of the 1997 IEEE Frequency Control Symposium.
- [2] W. A. Edson, Vacuum Tube Oscillators, John Wiley & Sons, 1953, pp 212-218.
- [3] Ibid, pp. 205-208.
- [4] Ibid, pp. 142-151.
- [5] F. Butler, "Series-Resonant Crystal Oscillators," Wireless Engineer, June, 1946, pp. 157-160.
- [6] J. R. Burgoon and R. L. Wilson, "SC-Cut Oscillator Offers Improved Performance," Hewlett-Packard Journal, March 1981, pp. 20-29.
- [7] L. A. Meacham, "Bridge-Stabilized Oscillator", Proc. IRE, Oct, 1938, pp. 1278-1294.
- [8] L. S. Ferris, "Transimpedance Oscillator Having High Gain Amplifier," U.S. Patent #4,358,742, Nov. 9, 1982.
- [9] T. A. Pendleton, A System for Precision Frequency Control of a 100 kc. Oscillator by Means of a Quartz-Crystal Resonator, M.S. Thesis, Univ. of Maryland, May 1953.
- [10] P. G. Sulzer, "High Stability Bridge Balancing Oscillator," Proc. IRE, June 1955, pp. 701-707.
- [11] M. E. Van Valkenburg, Introduction to Modern Network Synthesis, John Wiley & Sons, 1953, pp 337-338.
- [12] A. I. Zverev, Handbook of Filter Synthesis, John Wiley & Sons, 1967, pp 423-425.
- [13] J. R. Burgoon, "Crystal Oscillator Having Low Noise Signal Extraction Circuit," U.S. Patent # 4,283,691, Nov. 5, 1981.
- [14] A. Benjaminson, "A Crystal Oscillator With Bidirectional Frequency Control and Feedback ALC," in Proceedings of the 40th Annual Symposium on Frequency Control, 1986, pp. 344-349.
- [15] R.K. Karlquist, "Bridge-stablized oscillator circuit and method," U.S. Patent #5,708,394, Jan. 13, 1998.